Photoluminescence Tuning in Novel Bi^{3+}/Mn^{4+} Co-doped La_2ATiO_6:(A = Mg, Zn) Double Perovskite Structure: Phase Transition and Energy Transfer

Gongcheng Xing,[a] Yuxin Feng,[a] Min Pan,[a] Yi Wei,[a] Guogang Li,[a,*] Peipei Dang,[b] Sisi Liang,[b] Maxim S. Molokeev, [c, d, e] Ziyong Cheng,[b] Jun Lin[b, f, *]

[a]*Engineering Research Center of Nano-Geomaterials of Ministry of Education, Faculty of Materials Science and Chemistry, China University of Geosciences, 388 Lumo Road, Wuhan 430074, P. R. China*

[b]*State Key Laboratory of Rare Earth Resource Utilization, Changchun Institute of Applied Chemistry, Chinese Academy of Sciences, Changchun 130022, P. R. China*

[c]*Laboratory of Crystal Physics, Kirensky Institute of Physics, FRC KSC SB RAS, Krasnoyarsk 660036, Russia*

[d]*Department of Physics, Far Eastern State Transport University, Khabarovsk, 680021 Russia*

[e]*Siberian Federal University, Krasnoyarsk, 660041, Russia*

[f]*School of Applied Physics and Materials, Wuyi University, Jiangmen, Guangdong, 529020, P. R. China*

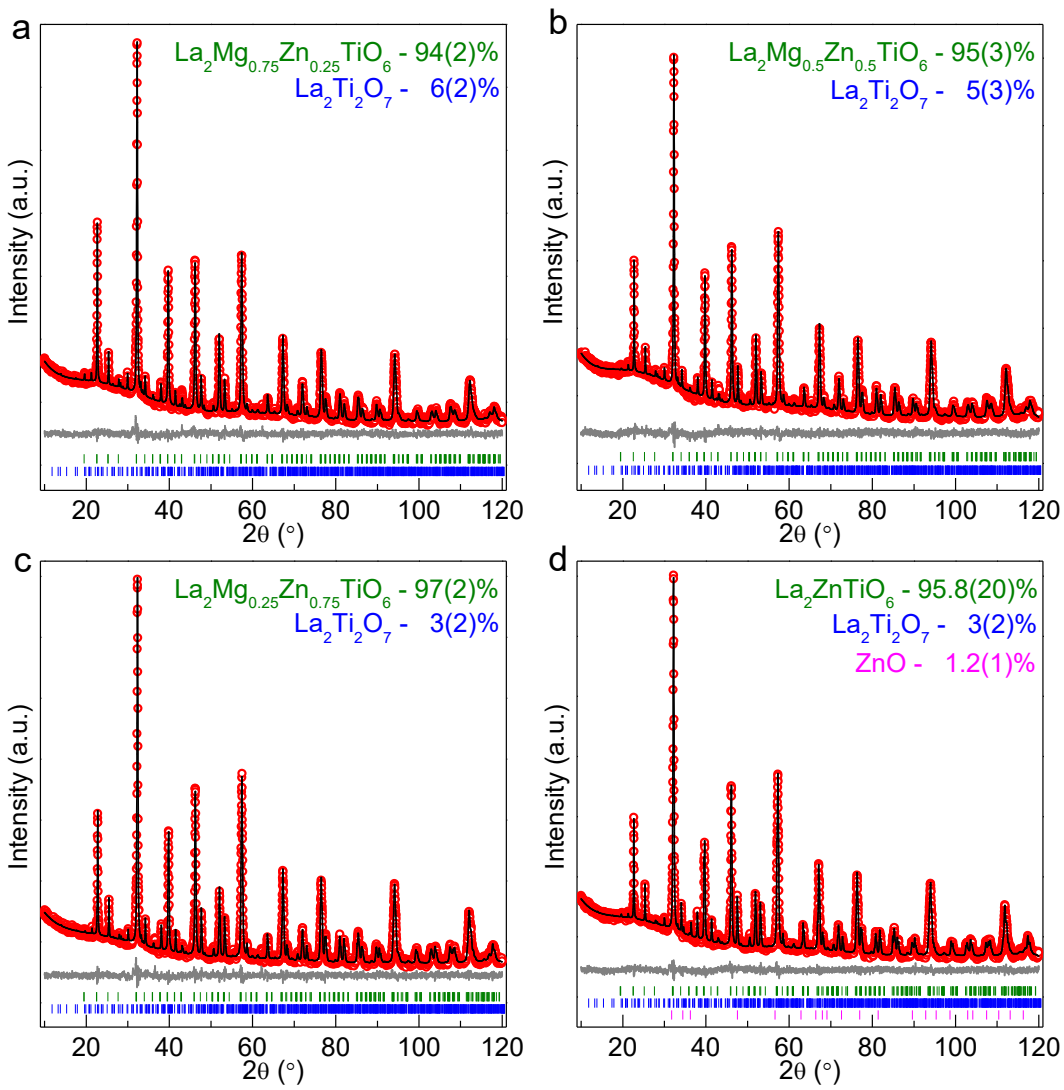

Figure S1. Difference Rietveld plot of $LM_{(1-w)}Z_w$:0.005Bi^{3+}, 0.002Mn^{4+}: (a) w = 0.25; (b) w = 0.5; (c) w = 0.75; (d) w = 1.

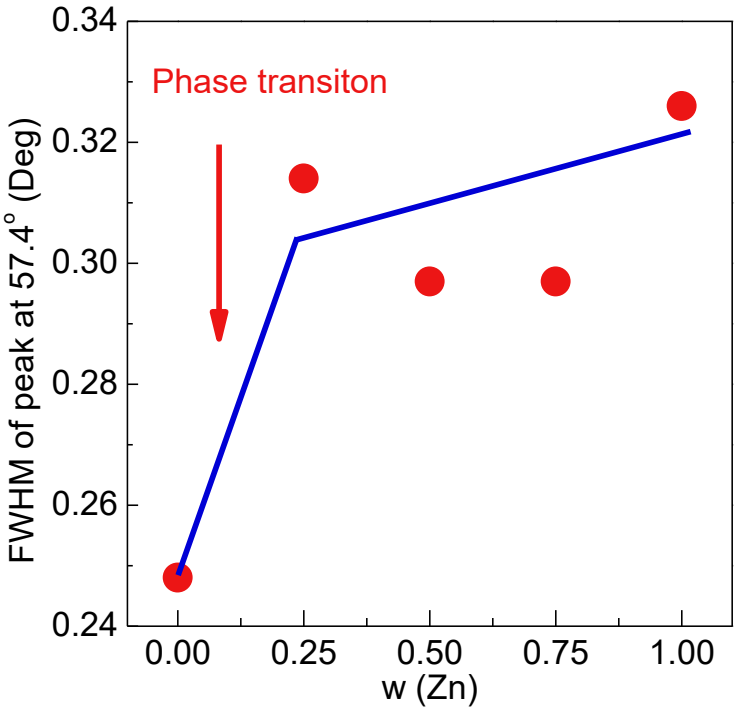

Figure S2. The FWHM of emission peak located at 2θ = 57.4° in $LM_{(1-w)}Z_w$:0.005Bi^{3+}, 0.002Mn^{4+} ($0 \leqslant w \leqslant 1$) samples. The obvious jump between $w = 0$ and $w = 0.25$ can be associated with the phase transition between *Pbnm* and $P2_1/n$ phases.

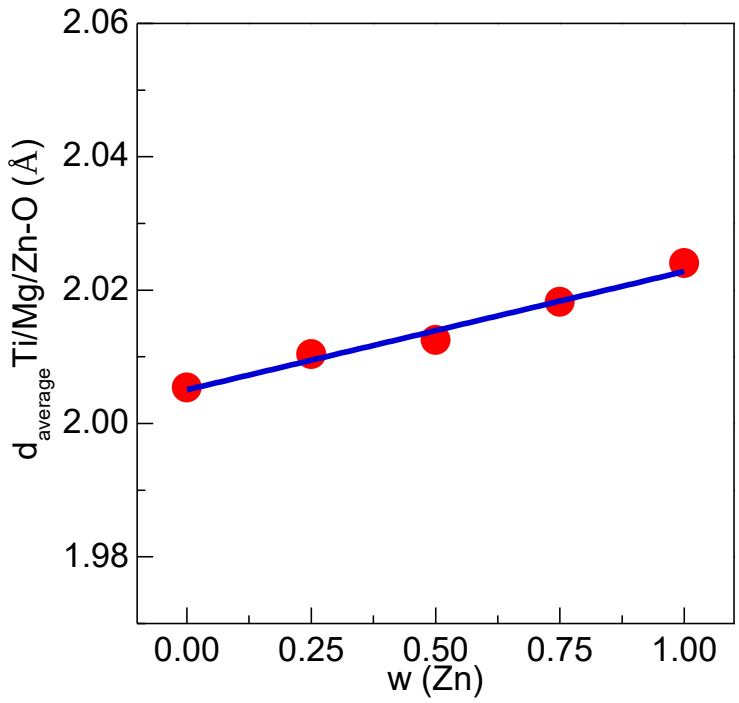

Figure S3. The average Ti/Mg/Zn-O bond length per Zn concentration value in $LM_{(1-w)}Z_wT$:0.005Bi^{3+}, 0.002Mn^{4+} ($0 \leq w \leq 1$).

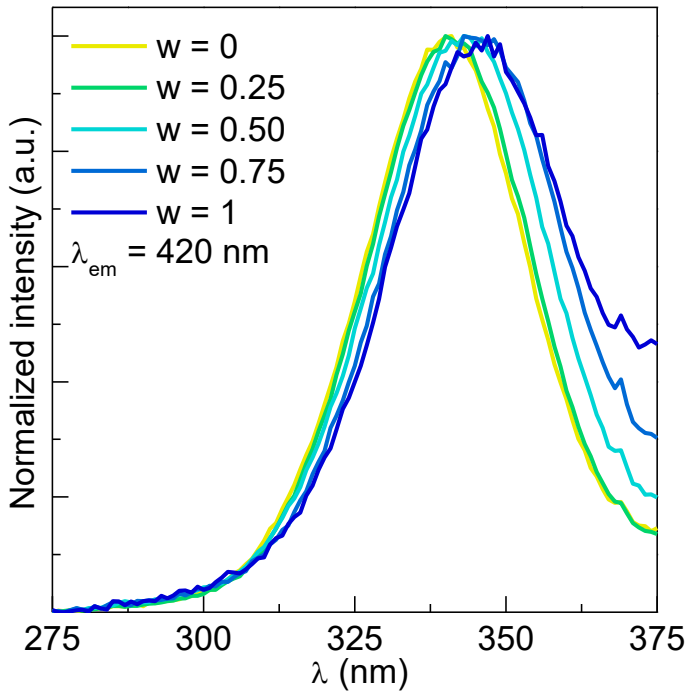

Figure S4. Normalized PLE spectra of $LM_{(1-w)}T_w$:0.005Bi^{3+}, 0.002Mn^{4+} ($0 \leq w \leq 1$) monitored at 420 nm for Bi^{3+}.

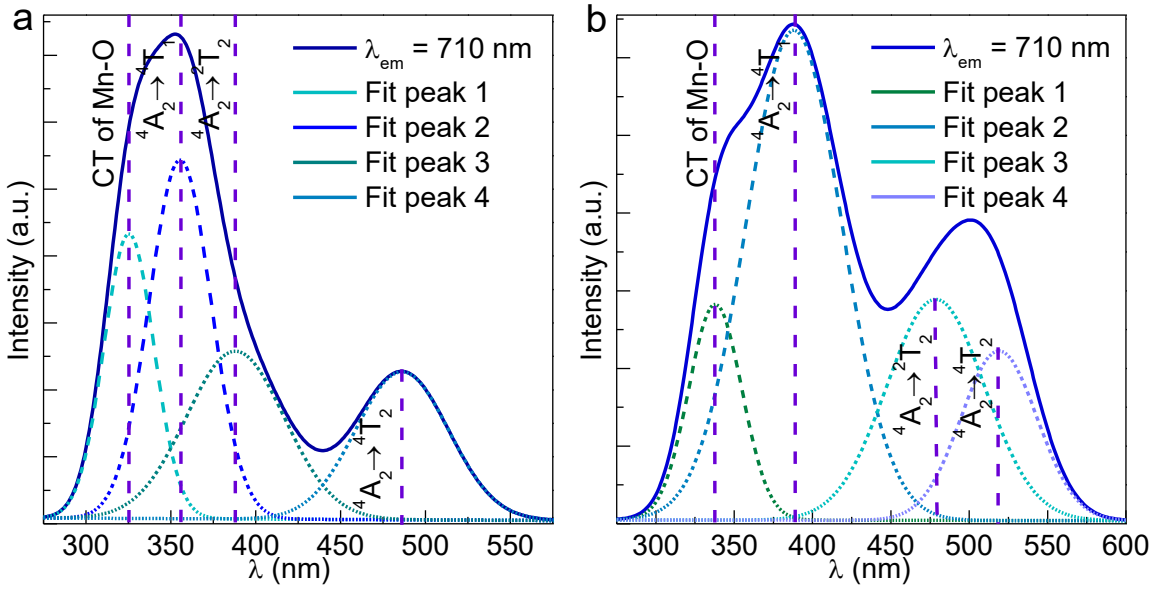

Figure S5. The Gaussian fitting of PLE spectra of (a) LMT:0.005Bi^{3+}, 0.002Mn^{4+} and (b) LZT:0.005Bi^{3+}, 0.002Mn^{4+}.

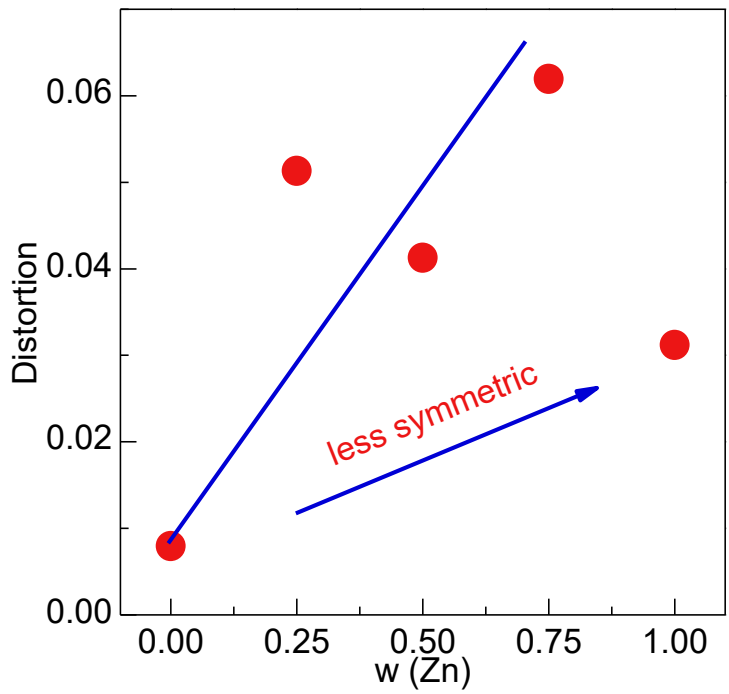

Figure S6. The CF distortion of [Ti/Zn/Mg)O_6] polyhedron as a function of Zn^{2+} concentrations.

$$D = \frac{1}{N}\sum_{i=1}^{n}\frac{|d_i - d_{av}|}{d_{av}}$$

where D represents the lattice distortion, d_i is the distance from Ti/Zn/Mg to the ith coordinating O atoms, d_{av} is the average Ti/Zn/Mg–O distance, and N is the coordination numbers.

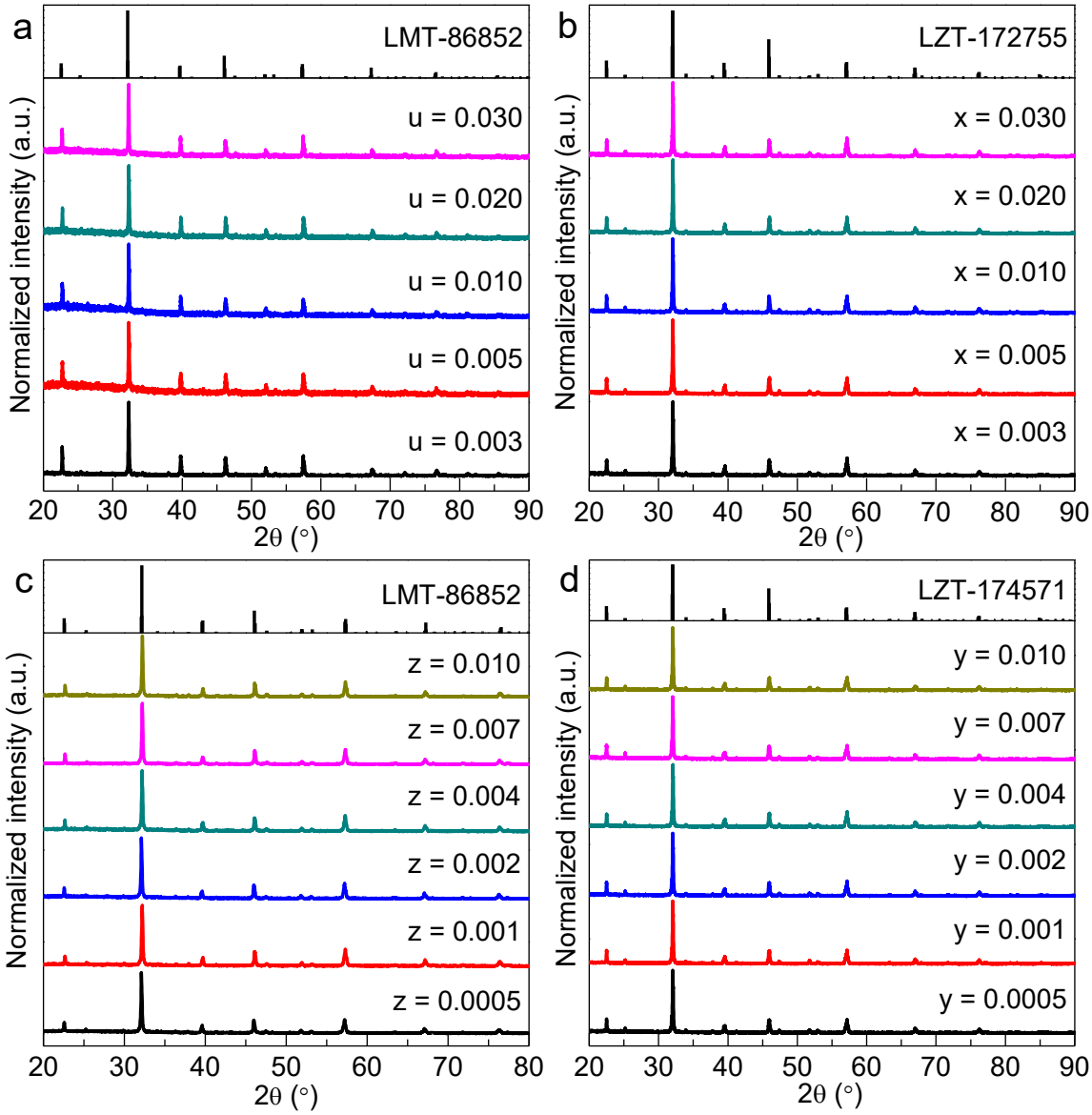

Figure S7. XRD patterns of (a) $L_{(1-u)}MT:uBi^{3+}$ ($0 \leq u \leq 0.03$); (b) $L_{(1-x)}ZT:xBi^{3+}$ ($0 \leq x \leq 0.03$); (c) $LMT_{(1-z)}:0.005Bi^{3+}, zMn^{4+}$ ($0 \leq z \leq 0.01$); (d) $LZT_{(1-y)}:0.005Bi^{3+}, yMn^{4+}$ ($0 \leq y \leq 0.01$).

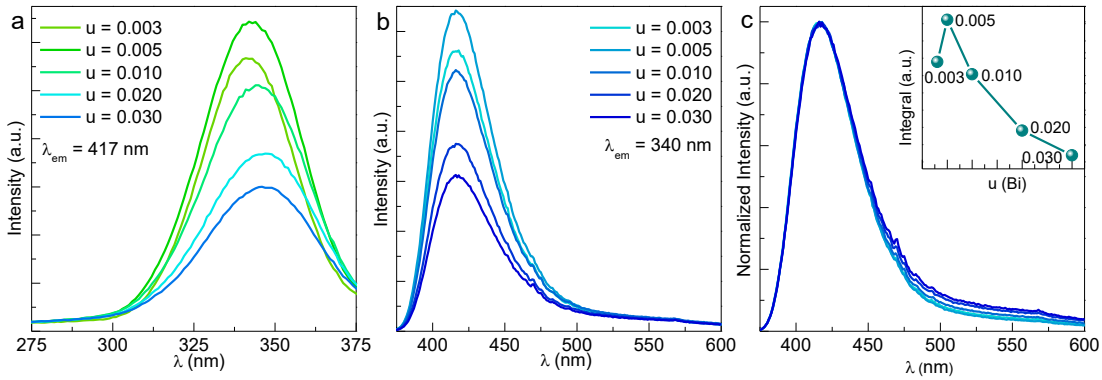

Figure S8. (a) PLE (monitored at 417 nm), (b) PL (excited at 340 nm) and (c) Normalized PL spectra and integrated intensity of $L_{(1-u)}MT:uBi^{3+}$ ($0 \leq u \leq 0.03$) as a function of Bi^{3+} ions.

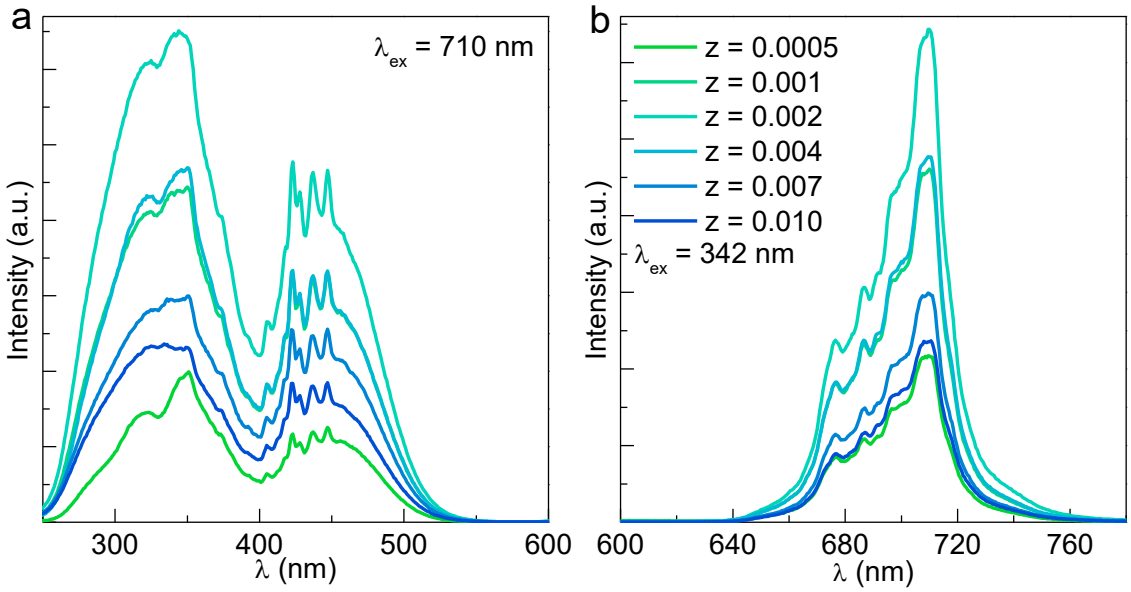

Figure S9. (a) PLE (monitored at 710 nm) and (b) PL (excited at 342 nm) spectra of $LMT_{(1-z)}$:0.005Bi^{3+}, zMn^{4+} ($0 \leq z \leq 0.01$).

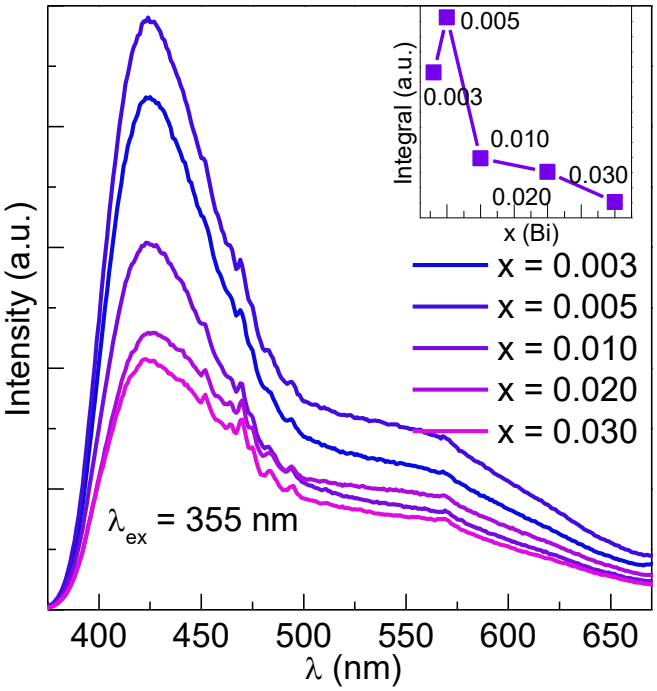

Figure S10. PL spectra and integrated intensity as a function of Bi^{3+} concentrations of $L_{(1-x)}ZT:xBi^{3+}$ ($0 \leq x \leq 0.03$).

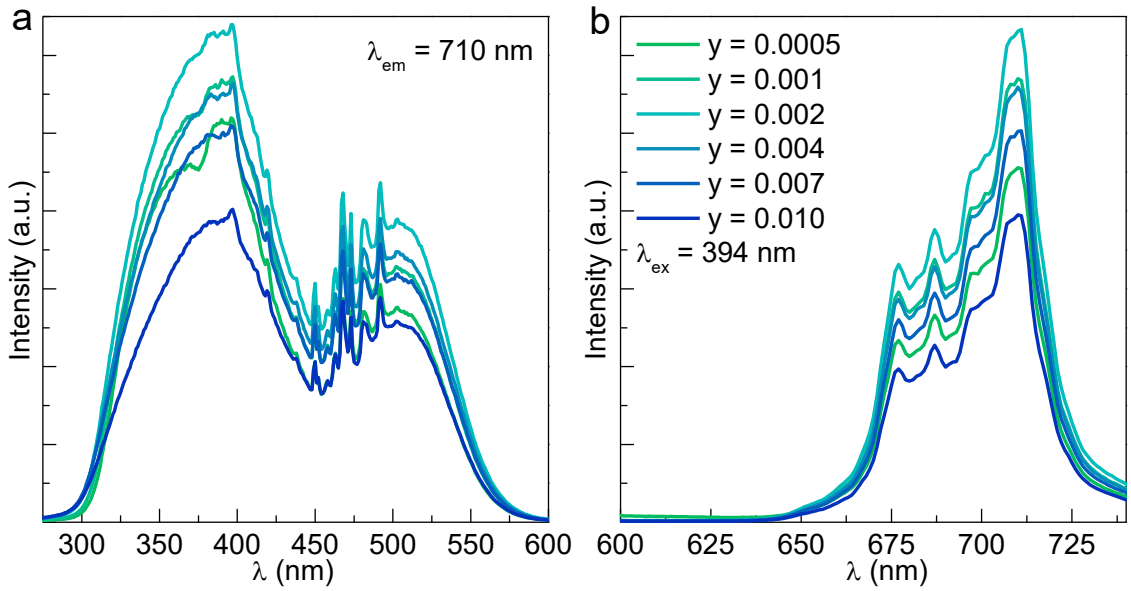

Figure S11. (a) PLE (monitored at 710 nm) and (b) PL (excited at 394 nm) spectra of $LZT_{(1-y)}$:0.005Bi^{3+}, $y$$Mn^{4+}$ ($0 \leq y \leq 0.01$).

Table S1. Fractional atomic coordinates and isotropic displacement parameters (Å^2) of $LM_{(1-w)}Z_wT$:0.005Bi^{3+},0.002Mn^{4+}.

Atom	*x*	*y*	*z*	B_{iso}	Occ.
			w = 0		
La	-0.0065 (3)	0.0242 (2)	0.25	1.04 (7)	1
Ti	0.5	0	0	0.15 (7)	0.5
Mg	0.5	0	0	0.15 (7)	0.5
O1	0.041 (2)	0.4898 (14)	0.25	0.92 (16)	1
O2	0.727 (2)	0.272 (2)	0.0528 (14)	0.92 (16)	1
			w = 0.25		
La	0.9949 (10)	0.0297 (2)	0.2492 (12)	0.76 (8)	1
Zn1	0	0.5	0	1.9 (4)	0.50 (46)
Mg1	0	0.5	0	1.9 (4)	0.50 (46)
Ti1	0	0.5	0	1.9 (4)	0.00 (91)
Ti2	0.5	0	0	0.3 (3)	1.00 (91)
Zn2	0.5	0	0	0.3 (3)	0.00 (46)
Mg2	0.5	0	0	0.3 (3)	0.00 (46)
O1	0.231 (7)	0.176 (7)	0.976 (5)	0.5 (3)	1
O2	0.288 (6)	0.724 (6)	0.956 (5)	0.5 (3)	1
O3	0.428 (5)	0.984 (2)	0.243 (7)	0.5 (3)	1
			w = 0.5		
La	0.9950 (10)	0.0327 (2)	0.2484 (12)	0.88 (7)	1
Zn1	0	0.5	0	0.4 (8)	0.3 (15)
Mg1	0	0.5	0	0.4 (8)	0.3 (15)
Ti1	0	0.5	0	0.4 (8)	0.3 (29)
Ti2	0.5	0	0	0.5 (7)	0.7 (29)
Zn2	0.5	0	0	0.5 (7)	0.2 (15)
Mg2	0.5	0	0	0.5 (7)	0.2 (15)
O1	0.225 (9)	0.183 (8)	0.982 (5)	0.5 (3)	1
O2	0.296 (6)	0.720 (7)	0.950 (5)	0.5 (3)	1
O3	0.426 (5)	0.981 (2)	0.245 (10)	0.5 (3)	1
			w = 0.75		
La	0.9953 (9)	0.03392 (18)	0.2508 (14)	0.80 (7)	1
Zn1	0	0.5	0	0.2 (4)	0.57 (10)
Mg1	0	0.5	0	0.2 (4)	0.188 (35)
Ti1	0	0.5	0	0.2 (4)	0.25 (14)
Ti2	0.5	0	0	0.6 (5)	0.75 (14)
Zn2	0.5	0	0	0.6 (5)	0.18 (10)
Mg2	0.5	0	0	0.6 (5)	0.062 (35)
O1	0.241 (6)	0.183 (6)	0.974 (5)	0.5 (2)	1
O2	0.310 (5)	0.725 (7)	0.965 (4)	0.5 (2)	1
O3	0.417 (4)	0.9863 (18)	0.248 (7)	0.5 (2)	1
			w = 1		
La	0.9936 (7)	0.03470 (14)	0.2498 (10)	0.99 (6)	1
Zn1	0	0.5	0	0.7 (4)	0.849 (57)
Ti1	0	0.5	0	0.7 (4)	0.151 (57)
Ti2	0.5	0	0	0.6 (5)	0.849 (57)
Zn2	0.5	0	0	0.6 (5)	0.151 (57)
O1	0.228 (7)	0.206 (7)	0.965 (5)	1.0 (2)	1
O2	0.290 (6)	0.723 (7)	0.949 (5)	1.0 (2)	1
O3	0.422 (3)	0.9854 (16)	0.240 (5)	1.0 (2)	1

Table S2. Main bond lengths (Å) of $LM_{(1-w)}Z_wT$:0.005Bi^{3+},0.002Mn^{4+}

		w = 0	
La—O1	2.602 (8)	La—O2^{ii}	2.420 (12)
La—O1^{i}	2.982 (8)	La—O2^{vi}	2.937 (11)
La—O1^{ii}	2.593 (12)	(Ti/Mg)—O1^{ii}	1.9802 (14)
La—O1^{iii}	2.974 (12)	(Ti/Mg)—O2	2.012 (12)
La—O2^{iv}	2.551 (11)	(Ti/Mg)—O2^{vii}	2.020 (12)
La—O2^{v}	3.288 (11)		
		w = 0.25	
La—O1^{i}	2.65 (4)	La—O3^{viii}	2.43 (3)
La—O1^{ii}	2.46 (4)	La—O3^{ix}	2.570 (12)
La—O1^{iii}	3.30 (4)	La—O3^{x}	3.079 (12)
La—O1^{iv}	2.84 (4)	(Zn1/Mg1/Ti1)—O1^{xi}	2.23 (4)
La—O2^{v}	3.30 (4)	(Zn1/Mg1/Ti1)—O2^{xi}	2.06 (3)
La—O2^{vi}	2.64 (4)	(Zn1/Mg1/Ti1)—O3^{xii}	2.06 (5)
La—O2^{iii}	2.83 (4)	(Zn2/Mg2/Ti2)—O1^{xi}	1.80 (4)
La—O2^{iv}	2.45 (4)	(Zn2/Mg2/Ti2)—O2^{xiii}	1.97 (3)
La—O3^{vii}	3.17 (3)	(Zn2/Mg2/Ti2)—O3^{vii}	1.96 (5)
		w = 0.5	
La—O1^{i}	2.60 (4)	La—O3^{viii}	2.545 (14)
La—O1^{ii}	2.50 (4)	La—O3^{ix}	3.114 (13)
La—O1^{iii}	2.86 (4)	(Zn1/Mg1/Ti1)—O1^{x}	2.17 (4)
La—O2^{iv}	2.65 (4)	(Zn1/Mg1/Ti1)—O2^{x}	2.09 (4)
La—O2^{v}	2.84 (4)	(Zn1/Mg1/Ti1)—O3^{xi}	2.05 (8)
La—O2^{iii}	2.40 (4)	(Zn2/Mg2/Ti2)—O1^{x}	1.85 (5)
La—O3^{vi}	3.18 (3)	(Zn2/Mg2/Ti2)—O2^{xii}	1.98 (4)
La—O3^{vii}	2.42 (3)	(Zn2/Mg2/Ti2)—O3^{vi}	1.98 (8)
		w = 0.75	
La—O1^{i}	2.71 (4)	La—O3^{viii}	2.37 (2)
La—O1^{ii}	2.52 (4)	La—O3^{ix}	2.578 (11)
La—O1^{iii}	3.27 (4)	La—O3^{x}	3.103 (11)
La—O1^{iv}	2.76 (4)	(Zn1/Mg1/Ti1)—O1^{xi}	2.23 (3)
La—O2^{v}	3.34 (3)	(Zn1/Mg1/Ti1)—O2^{xi}	2.16 (3)
La—O2^{vi}	2.76 (3)	(Zn1/Mg1/Ti1)—O3^{xii}	2.04 (5)
La—O2^{iii}	2.71 (3)	(Zn2/Mg2/Ti2)—O1^{xi}	1.78 (3)
La—O2^{iv}	2.45 (3)	(Zn2/Mg2/Ti2)—O2^{xiii}	1.89 (3)
La—O3^{vii}	3.24 (2)	(Zn2/Mg2/Ti2)—O3^{vii}	2.01 (5)
		w = 1	
La—O1^{i}	2.78 (4)	La—O3^{viii}	2.408 (18)
La—O1^{ii}	2.49 (4)	La—O3^{ix}	2.571 (10)
La—O1^{iii}	3.30 (4)	La—O3^{x}	3.116 (9)
La—O1^{iv}	2.68 (4)	(Zn1/Ti1)—O1^{xi}	2.10 (4)
La—O2^{v}	3.38 (4)	(Zn1/Ti1)—O2^{xi}	2.08 (4)
La—O2^{vi}	2.61 (4)	(Zn1/Ti1)—O3^{xii}	2.10 (4)
La—O2^{iii}	2.87 (4)	(Zn2/Ti2)—O1^{xi}	1.92 (4)
La—O2^{iv}	2.42 (4)	(Zn2/Ti2)—O2^{xiii}	1.99 (4)
La—O3^{vii}	3.198 (18)	(Zn2/Ti2)—O3^{vii}	1.95 (4)

Symmetry codes:

for *w* = 0 sample (i) *x*, *y*-1, *z*; (ii) -*x*+1/2, *y*-1/2, -*z*+1/2; (iii) -*x*-1/2, *y*-1/2, -*z*+1/2; (iv) *x*-1, *y*, *z*; (v) -*x*+1, -*y*, -*z*; (vi) *x*-1/2, -*y*+1/2, -*z*; (vii) -*x*+3/2, *y*-1/2, *z*.

for *w* ≥ 0.25 samples (i) *x*+1, *y*, *z*-1; (ii) -*x*+1, -*y*, -*z*+1; (iii) -*x*+3/2, *y*-1/2, -*z*+3/2; (iv) *x*+1/2, -*y*+1/2, *z*-1/2; (v) *x*+1, *y*-1, *z*-1; (vi) -*x*+1, -*y*+1, -*z*+1; (vii) *x*, *y*-1, *z*; (viii) *x*+1, *y*-1, *z*; (ix) -*x*+3/2, *y*-1/2, -*z*+1/2; (x) -*x*+3/2, *y*-3/2, -*z*+1/2; (xi) *x*, *y*, *z*-1; (xii) -*x*+1/2, *y*-1/2, -*z*+1/2; (xiii) *x*, *y*-1, *z*-1.